Acta Cryst. (1995). A51, 271–288

The Validity of Form-Factor, Modified-Form-Factor and Anomalous-Scattering-Factor Approximations in Elastic Scattering Calculations

BY LYNN KISSEL

Computational Physics Group, L Division, Lawrence Livermore National Laboratory, Livermore, CA 94551, *USA, and Department of Physics and Astronomy, University of Pittsburgh, Pittsburgh, PA* 15260, *USA*

B. ZHOU*

Department of Physics and Astronomy, University of Pittsburgh, Pittsburgh, PA 15260, *USA*

S. C. ROY

Department of Physics, Bose Institute, Calcutta 700 009, *India*

S. K. SEN GUPTA

North Bengal University, Darjeeling 734 430, *India*

AND R. H. PRATT

Department of Physics and Astronomy, University of Pittsburgh, Pittsburgh, PA 15260, *USA*

(*Received* 11 *November* 1993; *accepted* 15 *August* 1994)

Abstract

The validity of form-factor, modified-form-factor and anomalous-scattering-factor approximations in predictions of elastic photon–atom scattering is assessed with the aid of the state-of-the-art numerical calculation of Rayleigh scattering obtained using the second-order S-matrix theory, in the photon energy range from 100 eV to 1 MeV. A comparison is made with predictions from S-matrix theory in the same atomic model for representative low-Z (carbon, $Z = 6$) and high-Z (lead, $Z = 82$) elements to get a general idea of the validity of these simpler more approximate methods. The importance of bound–bound contributions and the angle dependence of the anomalous scattering factors is discussed. A prescription is suggested, with the assumption of angle independence, that uses simpler approaches to obtain the elastic scattering cross sections in the soft-X-ray regime at the level of accuracy of the S-matrix calculation, failing at large momentum transfers for high-Z elements. Predictions from this prescription are compared with experiment. With starting point the many-body elastic scattering amplitude, a detailed discussion is presented of the partition of the elastic scattering amplitude into Rayleigh and Delbrück scattering components. This partition of the optical theorem reveals contributions from bound–bound atomic transitions, bound pair annihilation and bound pair production that are not usually associated with elastic scattering. In the partitioned optical theorem for Rayleigh scattering, as in the many-body optical theorem for scattering from excited states, subtracted cross sections naturally appear. These terms are needed, in addition to the familiar terms for photoionization, to relate the real and imaginary parts of the scattering amplitude.

* Present address: 395 Henry Street, Apartment 1N, Brooklyn, New York 11201, USA.

1. Introduction

Elastic scattering of photons by atoms, molecules and solids is an important method of obtaining information about structural properties of materials. To understand the elastic scattering from a composite system, elastic scattering from the basic unit (an isolated atom or ion) must be accurately known. By identification of the deviation of elastic scattering by a complex system from elastic scattering by free atoms, valuable information about how the complex system is organized can be retrieved. In particular, accurate knowledge of the scattering near the photoeffect absorption edges enables one to determine the structures of macromolecules (see, for example, Karle, 1989).

The second-order S-matrix approach (SM; see, for example, Kissel, Pratt & Roy, 1980) provides a better calculation of elastic scattering than is normally available from simpler approaches, namely the form-factor and anomalous-scattering-factor approximations. In this report, we use SM predictions to investigate the validity of simpler approximations to scattering and conclude that, in the independent particle approximation (IPA), the use of angle-independent anomalous scattering factors with a

modified relativistic form factor (MF+ASF) provides a fairly good approximation to SM in many cases. (Almost all current predictions of elastic scattering are done within IPA.) We use this insight into the validity of the MF+ASF approach to illustrate predictions that go beyond IPA, although the database does not now exist to support more systematic tabulations.

An isolated atom itself is a composite system of a nucleus and bound electrons. It is a good approximation to consider the elastic photon scattering by an atom as the coherent sum of contributions of elastic photon scattering from the nucleus (nuclear Thomson and nuclear resonance scattering) and of the bound electrons (Rayleigh scattering) and vacuum fluctuations (Delbrück scattering) in the field of the nucleus. At lower photon energies, the elastic scattering from bound atomic electrons gives the dominant contribution to the elastic photon–atom scattering amplitude. Nuclear Thomson scattering becomes important with increasing atomic number Z and becomes relatively important compared to Rayleigh scattering at large scattering angles and high photon energy. Nuclear resonance and fluctuation effects become significant only at higher photon energies. (Delbrück effects start to show up even for photon energies as low as about 600 keV.) An accurate calculation of Rayleigh scattering is generally quite complicated. In this work, we review some approximate but simpler approaches in calculating atomic Rayleigh scattering and assess their usefulness in application by comparing their predictions with results from more accurate calculations in the same potential model.

Up to now, most calculations of Rayleigh scattering have been simply performed within the framework of the independent-particle approximation (IPA), in which all atomic electrons are assumed to move independently in a common central potential due to the nuclear charge and to the average distribution of all electrons. IPA is a good approximation for photon energies that are not too low. But when photon energy is very low (as in the optical range) or very close to photoeffect thresholds (the regions of extreme anomalous scattering), many-electron correlation effects, which are neglected in IPA, become important and IPA becomes inadequate. Even though there have been some works that studied correlation effects (Lin, Cheng & Johnson, 1975; Ice, Chen & Crasemann, 1978; Roy, 1991; Zhou, Kissel & Pratt, 1992*b*), how to go beyond IPA to include the many-electron correlation effects in Rayleigh-scattering calculation is still an open question.

At present, the best available calculation of Rayleigh scattering from first principles within IPA is based on the code developed by Kissel (1977), which uses the second-order S-matrix method. Agreement with its predictions is observed in comparison with experimental results over a wide range of photon energies (Kane, Kissel, Pratt & Roy, 1986), not too near photoeffect thresholds (which are displaced from their experimental locations). The method requires a considerable amount of computation time, especially for heavy atoms and for high photon energies, which makes extensive systematic computation too expensive to perform. In addition, inclusion of effects beyond the IPA will be difficult within the currently implemented S-matrix codes.

A simpler but useful approach, which has been widely used in estimating the Rayleigh-scattering cross section, is the form-factor approximation (FF) or its improved version, the modified relativistic form factor (MF). [In subsequent discussions, we often distinguish between the nonrelativistic (NF) and relativistic (RF) versions of the form factor. Here, we generally concentrate on RF, so that all comparisons can be carried out completely within a single atomic model.] As less computer time is involved in form-factor calculations, extensive tabulations of NF, RF and MF are readily available for the elements $Z = 1$–100 (NF: Hubbell, Veigele, Briggs, Brown, Cromer & Howerton, 1975; RF: Hubbell & Øverbø, 1979; MF: Schaupp, Schumacher, Smend & Rullhusen, 1983). NF, RF and MF are small-momentum-transfer high-energy approximations and one expects substantial deviations for photon energies near and below the photoeffect thresholds, as well as for heavy elements and large momentum transfers. By the introduction of electron binding effects into the form factor, the MF produces better high-energy results for heavy elements and, more importantly, gives the correct relativistic high-energy limit for forward scattering (Kissel & Pratt, 1990).

To remedy the failure of RF or MF at low photon energies, anomalous scattering factors are often introduced, which correct RF or MF for forward-angle scattering. Dispersion relations (relating the real and imaginary parts of the forward-scattering amplitude) and the optical theorem (relating the imaginary forward-angle scattering amplitude to the photoabsorption cross section) have been used to obtain the anomalous scattering factors from photoabsorption data (Cromer & Liberman, 1970*a*,*b*, 1976, 1981; Cromer, 1974, 1983; Henke, Lee, Tanaka, Shimabukuro & Fujikawa, 1981, 1982; Henke, Gullikson & Davis, 1993). Usually only bound–free photoabsorption (photoionization) cross sections are used.

Once having these anomalous scattering factors for forward scattering, and taking them as a deviation (assumed angle-independent) from form-factor approximation at all angles, one can combine the anomalous scattering factors with RF or MF to calculate Rayleigh-scattering cross sections at finite angles (ASF approximation). As we show later, this approach does not generally give the same accuracy as the S-matrix calculation, and the angle-independent approximation will not be adequate at large momentum transfers, but it improves RF or MF substantially to give very good results at low photon energies. It is to be noted that the inclusion of anomalous terms with the RF or MF requires

very little additional computation time (once the anomalous scattering factors have been suitably tabulated).

As we begin to write out explicit expressions for scattering amplitudes, the reader should be alerted to the different sign conventions that are in common use in the literature. One convention involves the overall sign choice of the scattering amplitude. As the Thomson scattering amplitude is negative, some authors have explicitly factored out an overall minus sign (see, for example, James, 1962), while others have not (see, for example, Sakurai, 1967). A second important choice lies in the form of the photon wavefunction. The choice typically made in the physics literature, $\exp(i\mathbf{K}\cdot\mathbf{r}-i\omega t)$, differs from that made in the crystallographic literature, $\exp[-(i\mathbf{K}\cdot\mathbf{r}-i\omega t)]$, with a consequent difference in the relative signs of the real and imaginary parts of the scattering amplitude. We do not factor out the overall minus sign in our scattering amplitude A, and we use the plane-wave convention of the physics literature. We note the differences from the crystallographic literature in our final results for the anomalous scattering factors.

In this work, we compare the simpler approaches (namely the RF, MF and ASF approximations) with the more sophisticated second-order S-matrix calculation, for representative low-Z (carbon, $Z = 6$) and high-Z (lead, $Z = 82$) elements, so as to obtain a general idea of the validity of form factors with and without anomalous corrections. To ensure a consistent comparison, all calculations have been performed in the same atomic potential, the relativistic Hartree–Fock–Slater potential with the Latter tail (see, for example, Liberman, Cromer & Waber, 1971). The present work is organized as follows: in §2 we describe the best available first-principle calculation of atomic Rayleigh scattering, the second-order S-matrix method. In §3, the accuracy of RF approximation is discussed; §4 is devoted to the similar discussion for MF. The use of ASF is described in §5. Here we discuss some related issues, such as the high-energy limit, the angle-independent assumption and the contribution from bound–bound transitions. We make systematic comparisons of cross sections, obtained with the modified form factor combined with angle-independent anomalous scattering factors (MF+ASF), with the S-matrix calculations. Possible ways of calculating Rayleigh scattering beyond the IPA level are discussed in §6. In §7, we conclude by giving a practical prescription, based on these discussions, which uses simpler approaches, to obtain accurate Rayleigh-scattering cross sections at the level of accuracy of the S-matrix calculation for most cases of interest in the soft-X-ray regime.

2. The second-order S-matrix method

In the discussion that follows, elastic photon scattering from isolated atoms or ions is understood as scattering from many-particle systems of electrons and nucleons that are held together by electromagnetic and nuclear forces. In addition to these particles, in the language of hole theory, the atomic system includes a filled negative-energy sea for each kind of particle. We do not consider the forces (including those from radiation fields) that correlate motions of these particles. [The reader is referred to Pratt, Kissel & Bergstrom (1994) for discussion of inelastic photon–atom scattering – bound-electron Compton scattering.]

The interaction of radiation with this atomic system of particles and seas is described by introducing in the many-particle Hamiltonian the minimal electromagnetic coupling that, for each particle of charge q, replaces its momentum operator $\mathbf{p}$ by $\mathbf{p}-q\mathbf{A}/c$, with A the electromagnetic field at the coordinate of that particle. Then, the scattering of photons from this system of fermions (each satisfying a Dirac equation), to the lowest nonvanishing order in perturbation theory, is described by the second-order S-matrix amplitude (Fig. 1) as

$$A = -\sum_P [\langle N|O_f^*|P\rangle\langle P|O_i|N\rangle/(E_N - E_P + \hbar\omega + i0_+)] + [\langle N|O_i|P\rangle\langle P|O_f^*|N\rangle/(E_N - E_P - \hbar\omega - i0_+)], \quad (1)$$

where the elastic scattering cross section is computed as

$$d\sigma/d\Omega = |A|^2 \quad (2)$$

and $\hbar\omega$ is the energy of the incident (or scattered) photon, the operator O_i (O_f^*) describes the absorption (emission) of the incident (scattered) photon, $i = (-1)^{1/2}$, 0_+ is a small positive value and the states $|N\rangle$ and $|P\rangle$ are properly symmetrized solutions of the many-particle Dirac equation for noninteracting particles.

It is traditional to partition the amplitudes for scattering off an atomic system into amplitudes for scattering off its components – electrons, nucleons, the

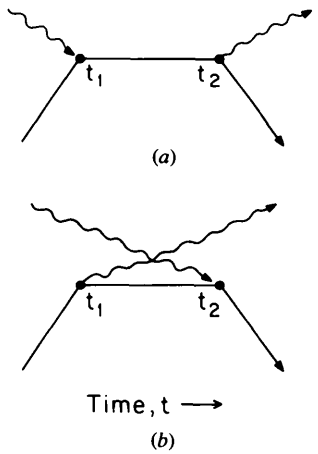

Fig. 1. Furry diagrams for second-order scattering. (*a*) Absorption first. (*b*) Emission first.

negative-energy seas – and, in the case of coherent elastic scattering (no energy transfer to, or change in, the internal degrees of freedom of the atomic system), call these the component amplitudes for Rayleigh (R), nuclear Thomson (T) and Delbrück (D) scattering (to be added coherently, since they cannot be distinguished in any observation):

$$A = A^R + A^T + A^D. \tag{3}$$

Pratt *et al.* (1994) present a more detailed discussion of this partitioning and the steps needed to reduce the many-particle scattering problem to a single-particle description of scattering. As far as we are aware, this is the first such discussion at a many-particle level; it also provides an explanation of why in a single-particle formalism one sums over a complete set of intermediate states, even though some of them are occupied and inaccessible. An important result of that discussion is the realization that there will be a subtracted cross section associated with downward transitions into real unoccupied bound states (only for scattering from excited states) and also into the negative-energy continuum states; the latter can be identified with the cross section for positron annihilation with the electron of the given bound state.

To the lowest order in the fine structure constant, the optical theorem for Rayleigh scattering states that

$$\mathrm{Im}\, A^R(\omega, 0) = (\omega/4\pi c)(\sigma^{\mathrm{PE}} + \sigma^{\mathrm{BBT}+} - \sigma^{\mathrm{BBT}-} - \sigma^{\mathrm{BPA}}), \tag{4}$$

where σ^{PE} is the cross section for the photoeffect, $\sigma^{\mathrm{BBT}+}$ is the cross section for a transition from the initial state to an excited bound state of the system, $\sigma^{\mathrm{BBT}-}$ is the cross section for a transition from the initial state to a bound state of lower energy and σ^{BPA} is the cross section for bound-electron pair annihilation, wherein an initial hole in the negative-energy sea is filled by one of the initial bound electrons. A similar discussion applies to the Delbrück amplitude, in which, in addition to transitions from negative-energy electrons to the continuum (the ordinary pair-production cross section), we have to add cross sections for transitions to the filled and unfilled bound states (bound pair production, where the electron is created in a bound state).

In all the S-matrix work to date (except some nonrelativistic analytic point-Coulomb calculations), one has summed or averaged scattering over all magnetic states of a subshell, thereby not considering the magnetic scattering effects that are possible with a polarized or oriented target.

General considerations of rotational invariance and parity conservation allow the Rayleigh scattering amplitude to be written in the form

$$A^R = (\boldsymbol{\varepsilon}_i \cdot \boldsymbol{\varepsilon}_f^*)\mathcal{M}(\mathbf{K}_i \cdot \mathbf{K}_f) + (\boldsymbol{\varepsilon}_i \cdot \mathbf{K}_f)(\boldsymbol{\varepsilon}_f^* \cdot \mathbf{K}_i)\mathcal{N}(\mathbf{K}_i \cdot \mathbf{K}_f), \tag{5}$$

where $\mathcal{M}$ and $\mathcal{N}$ are complex functions of the scattering angle (they only depend on the inner product $\mathbf{K}_i \cdot \mathbf{K}_f$), and the atom has been assumed to be rotationally invariant (*i.e.* composed of filled subshells). Note only the first term contributes for forward scattering or in dipole or form-factor approximations discussed subsequently; through the X-ray regime it varies relatively slowly with energy. If we decompose the polarization vector into components parallel and perpendicular to the scattering plane (defined by vectors $\mathbf{K}_i$ and $\mathbf{K}_f$, as shown in Fig. 2),

$$\boldsymbol{\varepsilon}_i = \varepsilon_i^{\parallel}\hat{\boldsymbol{\varepsilon}}_i^{\parallel} + \varepsilon_i^{\perp}\hat{\boldsymbol{\varepsilon}}_i^{\perp}, \quad \boldsymbol{\varepsilon}_f = \varepsilon_f^{\parallel}\hat{\boldsymbol{\varepsilon}}_f^{\parallel} + \varepsilon_f^{\perp}\hat{\boldsymbol{\varepsilon}}_f^{\perp}, \tag{6}$$

it is easy to show that

$$A^R = \varepsilon_i^{\parallel}\varepsilon_f^{\parallel}A_{\parallel}^R + \varepsilon_i^{\perp}\varepsilon_f^{\perp}A_{\perp}^R, \tag{7}$$

where

$$A_{\parallel}^R = \mathcal{M}\cos\theta - \mathcal{N}\sin^2\theta, \quad A_{\perp}^R = \mathcal{M}. \tag{8}$$

(In this notation, $\boldsymbol{\varepsilon}_i$ is the polarization of the incident photon, $\hat{\boldsymbol{\varepsilon}}_i^{\parallel}$ is a unit vector that is parallel to the plane of scattering and perpendicular to $\mathbf{K}_i$, while $\hat{\boldsymbol{\varepsilon}}_i^{\perp}$ is a unit vector that is perpendicular to the plane of scattering and perpendicular to $\mathbf{K}_i$.) The scattering angle θ is the angle between $\mathbf{K}_i$ and $\mathbf{K}_f$ ($\theta = 2\Theta$, where Θ is the Bragg angle). The cross section for scattering of initially unpolarized photons where the polarization of the scattered photon is not observed is obtained by averaging over incident-photon polarizations and summing over scattered-photon polarizations:

$$\mathrm{d}\sigma/\mathrm{d}\Omega = \tfrac{1}{2}(|A_{\parallel}^R|^2 + |A_{\perp}^R|^2). \tag{9}$$

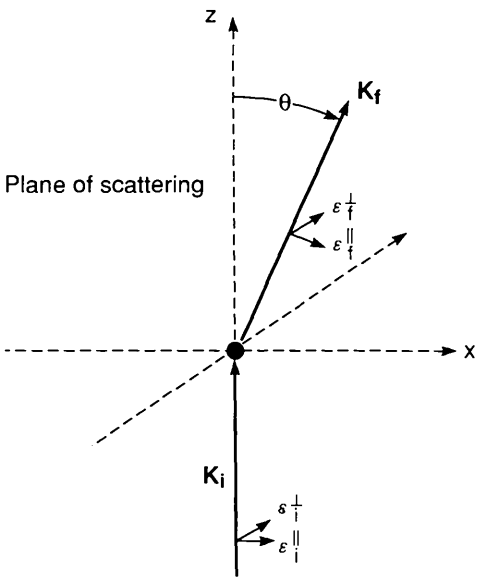

Fig. 2. Geometry of Rayleigh scattering. The XZ plane is chosen to be the plane of scattering.

The general case of polarized scattering is discussed by Roy, Sarkar, Pratt & Kissel (1986) in terms of Stokes parameters.

S-matrix Rayleigh-scattering calculations have been performed by Brown and co-workers (Brown, Peierls & Woodward, 1955; Brenner, Brown & Woodward, 1955; Brown & Mayers, 1956, 1957), Johnson and co-workers (Johnson & Feiock, 1968; Lin *et al.*, 1975; Johnson & Cheng, 1976), and Kissel & Pratt and co-workers (Kissel *et al.*, 1980; Kissel & Pratt, 1985; Kane *et al.*, 1986; Roy, Kissel & Pratt, 1983; Roy, Sarkar, Kissel & Pratt, 1987; Parker & Pratt, 1984; Smend, Schaupp, Czerwinski, Schumacher, Millhouse & Kissel, 1987; Zhou, Pratt, Roy & Kissel, 1990; Pratt *et al.*, 1994). Here, we do not discuss the detailed formalism of the numerical method, which can be found in Johnson & Feiock (1968) and Kissel (1977). Instead, we briefly describe the status of the SM method, since we use it as a reference to judge other approximate methods.

Results from the *S*-matrix calculation for Rayleigh scattering have been obtained and compared with experiments over a wide range of photon energies and elements (Kissel *et al.*, 1980; Kane *et al.*, 1986). Since threshold positions in the IPA SM calculation are somewhat different from actual experiment, simple scalings are sometimes applied in the comparison when the photon energy is near a threshold. As long as the photon energy is not too close to any thresholds, the SM predictions generally agree with experiments to within several percent. Because all significant multipoles and partial waves are included in the radiation interaction with the scattering electron in the atomic potential, the *S*-matrix method gives excellent results not only for low momentum transfers but also for large momentum transfers. In other words, the *S*-matrix method accurately predicts the angular distribution of Rayleigh scattering, even for very high photon energies. One major achievement of this method is that the accuracy at γ-ray energies is sufficiently high to enable an experimental identification of Delbrück scattering (Basavaraju, Kane & Varier, 1979; Mückenheim & Schumacher, 1980).

Published differential cross sections for elastic scattering using the *S*-matrix method are available as tables for seven photon energies in the range from 59.5 keV to 1.33 MeV for ten elements in the range $Z = 13$–103 (Kane *et al.*, 1986; see also Roy *et al.*, 1983); differential amplitudes are available for 2.754 MeV photons scattered by eight elements in the range $Z = 30$–92 for $\theta = 60$–$120°$ (Rullhusen, Mückenheim, Smend, Schumacher, Berg, Mork & Kissel, 1981); near-*K*-shell differential cross sections are available for $Z = 36$ and 54 for 21.2–43.7 keV (Smend *et al.*, 1987); polarization values for selected Z in the range 13–92 for photon energies from a few keV to above 1 MeV are available (Roy *et al.*, 1986); and fragmentary data are available throughout the X-ray regime (Kissel *et al.*, 1980; Zhou *et al.*, 1990). Unpublished SM values have been systematically computed for photon energies less than 300 times *K*-shell binding on a 52-point grid of energies of experimental interest in the range 0.0543–2754.1 keV for 38 neutral atoms in the range $Z = 1$–103; other scattered SM values are also available. (Contact LK for more information regarding these data.)

The evaluation of the *S*-matrix element is computer-intensive for heavy atoms and high photon energies, because more shells are involved in heavy atoms and more higher-multipole and partial-wave contributions are needed for high photon energies. However, the majority of the computational time is consumed in outer-shell calculations, while for large photon energies the contributions to the total Rayleigh scattering amplitude are mainly from inner shells. This allows us in many cases to use a faster, but still accurate, alternative approach: we can calculate inner shells using the *S*-matrix method, while estimating outer-shell amplitudes with a modified relativistic form factor (MF, which we discuss later), for photon energies large compared to the given outer-electron's binding energy. By doing so, we appreciably reduce computation time. For photon energies that are not large compared to a given outer-electron's binding energy, or for energies near to a bound–bound resonant transition (not included in MF) involving this given outer electron, this procedure will not be accurate.

It is important to mention that, while the Rayleigh scattering amplitude dominates at most angles for X-ray energies, other amplitudes in elastic photon scattering start to be important at higher energies. For light elements, the nuclear Thomson amplitude becomes important by 100 keV and dominates the large-angle scattering amplitude by 1 MeV. For heavy elements, the nuclear Thomson scattering becomes significant at back angles for energies about 500 keV, becomes comparable to the Rayleigh amplitude by 1 MeV and dominates at most angles at higher energies. The Delbrück amplitude begins to contribute at intermediate angles (about 60°) for energies somewhat below 1 MeV, and eventually dominates at most angles by 100 MeV (Kane *et al.*, 1986). In most situations considered here, the nuclear Thomson scattering amplitudes can be estimated from the following simple expressions:

$$A_{\parallel}^{\mathrm{NT}} = A_{\perp}^{\mathrm{NT}} \cos\theta, \quad A_{\perp}^{\mathrm{NT}} = -r_0(m/M)Z^2, \qquad (10)$$

where Z and M are the charge and mass of the nucleus, respectively. The unpolarized cross section including contributions from the Rayleigh and nuclear Thomson amplitudes is written as

$$\mathrm{d}\sigma/\mathrm{d}\Omega = \tfrac{1}{2}\left(\left|A_{\parallel}^{R} + A_{\parallel}^{\mathrm{NT}}\right|^2 + \left|A_{\perp}^{R} + A_{\perp}^{\mathrm{NT}}\right|^2\right). \qquad (11)$$

The nuclear Thomson amplitude makes relatively significant contributions to heavy atoms and it is included together with the Rayleigh scattering amplitude

in our subsequent comparisons for X-ray scattering to give the total elastic scattering amplitude; we have not included the Delbrück amplitude in this energy regime.

3. Form-factor approximation

In the limit of high photon energy and small momentum transfer, it can be shown that the Rayleigh scattering amplitude can be expressed as (Goldberger & Low, 1968; Zhou, 1991)

$$A^R \simeq -r_0 mc^2(\boldsymbol{\varepsilon}_i \cdot \boldsymbol{\varepsilon}_f^*)\sum_n \left[\langle n|\exp(-i\mathbf{K}\cdot\mathbf{r}) \times [E_n - V - c(\mathbf{K}\cdot\mathbf{p})]^{-1}|n\rangle\right], \quad (12)$$

where $\mathbf{K} = \mathbf{K}_f - \mathbf{K}_i \equiv \hbar\mathbf{q}$ is the momentum transfer and $\mathbf{p}$ is the electron momentum operator. This neglects $\mathcal{N}$ in (8).

Under the assumption that electrons in the atom are loosely bound to the nucleus, such that $\langle n|V|n\rangle$, $c\langle n||\mathbf{p}||n\rangle$ and $|E_n - mc^2|$ are all very much smaller than mc^2, the denominators in (12) may be replaced by the rest-mass energy of an electron, mc^2. Then, we get the Rayleigh scattering amplitude in the form-factor approximation [Franz (1935, 1936); Bethe, see Levinger (1952); Goldberger & Low (1968); Florescu & Gavrila (1976); for nonrelativistic derivations see, for example, Sommerfeld (1939); James (1962)]:

$$A^{\mathrm{FF}} = -r_0(\boldsymbol{\varepsilon}_i \cdot \boldsymbol{\varepsilon}_f^*)f(\mathbf{q}) \quad (13)$$

or, in terms of linear photon polarization,

$$A_{\parallel}^{\mathrm{FF}} = -r_0 f(\mathbf{q})\cos\theta, \quad A_{\perp}^{\mathrm{FF}} = -r_0 f(\mathbf{q}). \quad (14)$$

For Rayleigh scattering of an unpolarized photon, the differential cross section in form-factor (FF) approximation is

$$\mathrm{d}\sigma^{\mathrm{FF}}/\mathrm{d}\Omega = (r_0^2/2)|f(\mathbf{q})|^2(1+\cos^2\theta), \quad (15)$$

where θ is the scattering angle ($\theta = 2\Theta$, where Θ is the Bragg angle) and $f(\mathbf{q})$ is the Fourier transform of the electron charge density (see, for example, Hubbell *et al.*, 1975) for a momentum transfer $\hbar\mathbf{q}$.

In the special case of forward scattering ($\theta = 0$, $\hbar q = 0$), $f(0) = N$, where N is the total number of electrons in the atom. For a certain range of small q, $f_n(q)$ for a given subshell n will stay almost constant (equal to the number of electrons in the subshell) and then start to drop once q is large enough that $1/q$ is smaller than the size of the subshell. Thus, form factors of outer shells decrease earlier, at smaller momentum transfers, while form factors of inner shells drop at larger momentum transfers and the K-shell form factor drops last, for the form factor as considered a function of increasing q.

As already noted, extensive tabulations are available for atomic form factors, using both nonrelativistic wavefunctions (NF) and relativistic wavefunctions (RF). But one should not be misled by an impression that the relativistic form factor is necessarily better than the nonrelativistic one; there is theoretical and experimental evidence suggesting that the form factors obtained from relativistic wavefunctions can produce poorer predictions than those from nonrelativistic wavefunctions, particularly for heavy atoms (Roy *et al.*, 1983; Kane, Mahajani, Basavaraju & Priyadarshini, 1983). The reason might be that there is substantial cancellation among relativistic, retardation and higher-multipole effects, so that inclusion of relativistic effects but omission of other effects can make predictions worse. In general, both relativistic and nonrelativistic form factors differ from each other by no more than a few percent when the momentum transfer is not very large.

To examine the validity of RF approximation, we choose two representative neutral atoms: C ($Z = 6$) and

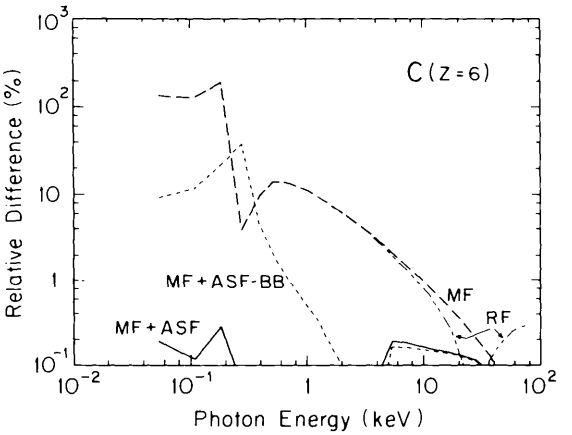

Fig. 3. Absolute relative difference in the total (angle-integrated) cross section for carbon as compared with SM: RF – relativistic form-factor approximation; MF – relativistic modified form-factor approximation; MF+ASF – MF with angle-independent anomalous scattering factors; MF+ASF–BB – MF+ASF neglecting bound–bound contributions to ASF. These curves also represent the differences in the forward-angle differential cross sections.

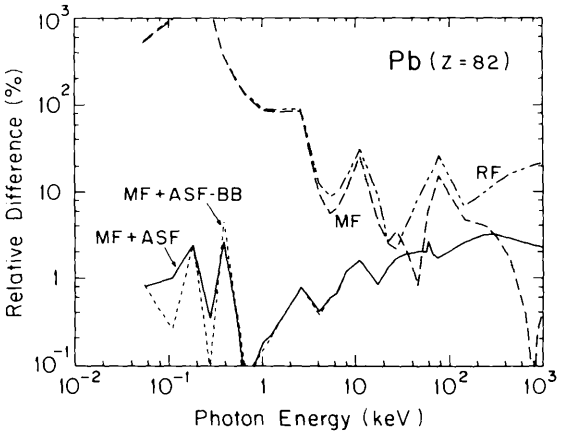

Fig. 4. Same as Fig. 3, for lead.

Pb ($Z = 82$). The form factors for these atoms were calculated using wavefunctions obtained in the relativistic Hartree–Fock–Slater potential with the Latter tail. We have compared the total (angle-integrated) cross section and the differential cross sections obtained in RF approximation, (11) [with the Rayleigh amplitude computed *via* (14)], with the SM results calculated in the same potential, for these atoms at various scattering angles. Relative difference curves of the angle-integrated total cross sections of Rayleigh scattering, comparing the RF approximation with SM, are shown in Figs. 3 and 4 for carbon and lead.

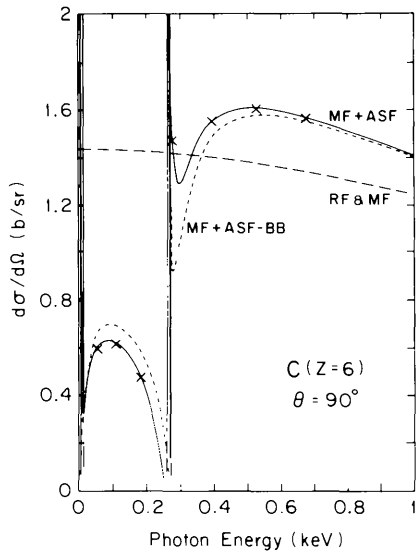

Fig. 5. Differential cross sections of Rayleigh scattering in various approximations near the K-shell photoeffect threshold of carbon (about 0.28 keV) for $\theta = 90°$. The crosses indicate SM values. The differences between RF and MF are indistinguishable on the scale of this plot.

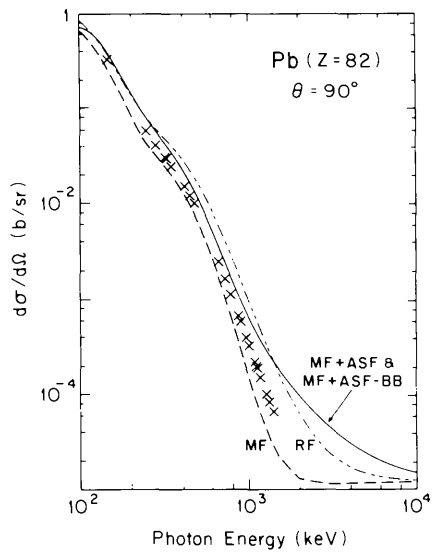

Fig. 6. Differential cross sections of Rayleigh scattering in various approximations at higher energies (larger momentum transfers) for lead for $\theta = 90°$. The crosses indiate SM values. The differences between MF+ASF and MF+ASF–BB are indistinguishable on the scale of this plot.

Figs. 3 and 4 also represent the quantitative error for the differential cross sections at $\theta = 0°$ (either there is little angle dependence in the difference of predictions or forward angles dominate the integrated cross section). Differential cross sections at $\theta = 90°$ for carbon and lead are shown in Figs. 5 and 6. Further quantitative comparisons are made in Fig. 7, which depicts the relative differences of differential cross sections between the RF and the SM calculations at three different angles, $\theta = 0$, 30 and 90°, for lead at higher energies. (There is little angle dependence in the difference curves at all energies for carbon, for lower energies for lead.) It can be seen that, for all elements, RF approximation gives, in general, good predictions in the forward direction for photon energies well above the K-shell photoeffect threshold but produces extremely poor results for photon energies close to and below the K-shell photoeffect threshold. As momentum-transfer becomes large (*i.e.* for high photon energies at large angles), RF also fails to predict the correct SM cross sections.

In general, we find that:

(i) The angle-integrated total cross section obtained in RF is good (errors less than about 10%) for photon energies above the K-shell photoeffect threshold, for all elements.

(ii) Above the K-shell photoeffect threshold, RF predictions for the differential cross section of Rayleigh scattering are very good (errors less than a few percent) in the forward direction for almost all elements. The error in the forward direction in the high-energy limit is larger for heavy atoms than for light atoms.

(iii) The differential cross section obtained in RF is good (errors less than about 10%) for all angles in light

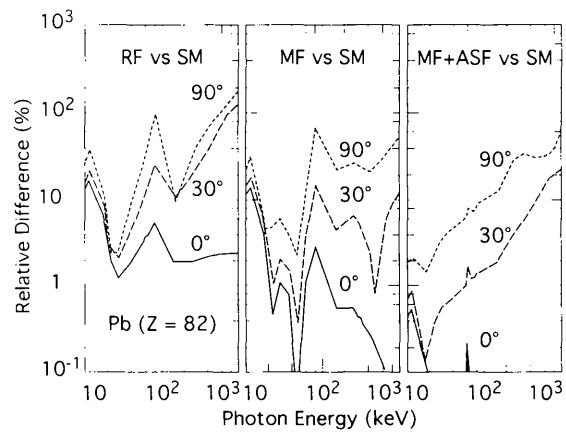

Fig. 7. Absolute difference in various approximations in comparison with the differential scattering cross sections in SM for lead at higher energies. At lower energies for lead, and at all energies for carbon, the relative difference curves show little angle dependence.

and medium elements and for small angles in heavy elements over a range of photon energies from somewhat above the K-shell photoeffect threshold to about ten times greater than this.

(iv) For photon energies near and below the K-shell photoeffect threshold, RF fails for both differential and total cross sections.

(v) For finite angles at very high photon energy, the differential cross section obtained in the RF approximation fails, especially for heavy atoms.

While our comparison was made explicitly with RF, we expect that these overall conclusions will be generally valid for all form-factor (FF) approximations, including NF (form factors computed using nonrelativistic wavefunctions).

In FF approximation, the bound electrons are treated as a continuous distribution of static free-electron charge fixed in space, with Thomson scattering from each element of charge as though associated with a single-electron mass. The phase differences in scattering from the differing positions of the charge are represented by the form factor, which is the Fourier transformation of the spatial charge density. When photon energies are well above the K-shell photoeffect threshold, the scattering occurs as off free electrons, and the FF approximation is better justified. FF works well at forward and small angles at high energies. But for photon energies comparable to the atomic binding energies, effects related to atomic structure, such as virtual excitation and ionization of atomic electrons, now play a more important role in the scattering process, creating rich structures in the cross section, especially for photon energies close to the edges. The FF approximation, which neglects such effects, fails to predict any of these structures. In particular, one sees that, near edges, FF performs much poorer than for other energies, owing to the dominance of contributions from virtual ionizations and excitations of electrons in those subshells.

For photon energies below the K-shell photoeffect threshold, the relative difference curves are almost independent of angle. This fact implies that the simple angular distribution given by (15), which basically corresponds to the assumption $\mathcal{N} \simeq 0$ in (5) and (8), is a reasonably good approximation in this photon-energy region, except very near edges (Parker & Pratt, 1984). However, as photon energy goes above the K-shell photoeffect threshold, the relative difference curves for different angles start to diverge from each other, while the curve for $\theta = 0$ remains close to 0. This indicates that the simple expression for the angular distribution is breaking down for large-momentum-transfer situations.

The relative error in FF at forward angle drops significantly above K-shell photoeffect thresholds with increasing Z, considered relative to K-shell binding energies, while for specified photon energy the reverse is true. For example, the error at twice the K-shell binding energy of lead (~88 keV) is about 10%, whereas, for carbon, only after about five times its K-binding energy (~280 eV) does the error become less than 10%.

The FF approximation gives generally good predictions for the total cross sections for photon energies above the K-shell threshold. For these energies, the Rayleigh amplitude rapidly decreases with increasing momentum transfer, as does the FF value. Consequently, the main contribution to the total cross section comes from near-forward scattering angles, where the FF approximation works well. Only a small contribution is made to the total cross section at finite angles, where the differential scattering cross section is not well predicted by the FF approximation.

4. Modified-form-factor approximation

An improvement to the form factor, known as the modified relativistic form factor, introduced first by Franz (1936), takes into account corrections due to electron binding. In the modifed form-factor (MF) approximation, $E_n - V(r)$ is retained and only the $c(\mathbf{K}\cdot\mathbf{p})$ term is dropped in (12). Hence, the Rayleigh scattering amplitude in MF approximation (assuming spherically symmetric charge densities ρ_n) is

$$A^{\mathrm{MF}} = -r_0(\boldsymbol{\varepsilon}_i \cdot \boldsymbol{\varepsilon}_f^*)g(q) \tag{16}$$

or, in terms of linear photon polarization

$$A_{\parallel}^{\mathrm{MF}} = -r_0 g(q)\cos\theta, \quad A_{\perp}^{\mathrm{MF}} = -r_0 g(q). \tag{17}$$

For Rayleigh scattering of an unpolarized photon, the differential cross section in MF approximation is

$$\mathrm{d}\sigma^{\mathrm{MF}}/\mathrm{d}\Omega = (r_0^2/2)|g(q)|^2(1+\cos^2\theta), \tag{18}$$

where θ is the scattering angle ($\theta = 2\Theta$, where Θ is the Bragg angle). The total-atom modified form factor is given as

$$g(q) = \sum_n g_n(q) = 4\pi \sum_n \int_0^\infty \rho_n(r)(\sin qr/qr)\left\{\frac{mc^2}{[E_n - V(r)]}\right\} r^2 \mathrm{d}r. \tag{19}$$

Unlike FF, owing to the presence of E_n, MF cannot be calculated directly from the total electron charge distribution; instead, contributions from electrons of each subshell must be calculated and summed. A complete tabulation of MF values was given by Schaupp, Schumacher, Smend & Rullhusen (1983), in which $g(q)$ for all elements in the Periodic Table were calculated using relativistic wavefunctions and potentials (total-atom and K-shell MF values are listed).

Comparisons of the MF approximation with the SM calculation are shown in Figs. 3 and 4 for the total (angle-integrated) cross section. Figs. 3 and 4 also represent the differences in the forward-angle differential cross sections as was discussed in the previous section. Further comparisons for the differential cross sections are shown in Figs. 5–7. We see that:

(i) Above the K-shell photoeffect threshold, MF predicts the differential cross section of Rayleigh scattering extremely well in the forward direction, apparently converging to the correct high-energy limit at infinite photon energy.

(ii) For photon energies near and below the K-shell photoeffect threshold, MF fails for both differential and total cross sections.

(iii) Above the K-shell photoeffect threshold, the errors in differential-cross-section predictions of MF for finite angles are about the same as those of FF.

(iv) MF works very well for the total cross section for photon energies above the K-shell photoeffect threshold; the improvement over FF reflects the improved forward-angle behavior.

The deviation of the MF approximation from the S-matrix calculation generally behaves similarly to that of the FF approximation, as discussed above. But one can see, from Figs. 3, 4 and 7, that the main improvement of the MF approximation is achieved for $\theta = 0$ and higher photon energies: MF reduces the relative error at forward angles from a few percent, as in the FF approximation, to a few tenths of a percent or less, as photon energy goes well above the K-shell photoeffect threshold. Although there is no formal proof, evidence such as this suggests that the relativistic MF gives essentially the correct high-energy limit of Rayleigh scattering in the forward direction.

5. Anomalous scattering factors

While the SM method is, in many cases, accurate in predicting Rayleigh scattering for X-ray and higher photon energies, it is often too expensive in terms of computer time for extensive systematic tabulation. On the other hand, the FF or MF approximations, though very simple and easy to compute, only work in limited situations and totally fail near and below the K-shell photoeffect threshold. A simple but more accurate method is needed. The use of anomalous scattering factors appears to provide such a method and we devote this section to a discussion of this approach.

(a) *Basic relations*

An important approach to the calculation of the amplitude $A(\omega, \theta)$ for elastic scattering, not requiring the assumption of IPA but in practice restricted to the case of forward scattering, utilizes the analytic nature of the forward scattering amplitude that follows from causality, leading to the dispersion relations

$$\mathrm{Re}\,A(\omega, 0) = (2\omega^2/\pi)\int_0^\infty [\mathrm{Im}\,A(\omega', 0)/\omega'(\omega'^2 - \omega^2)]\mathrm{d}\omega', \tag{20}$$

$$\mathrm{Im}\,A(\omega, 0) = (-2\omega/\pi)\int_0^\infty [\mathrm{Re}\,A(\omega', 0)/(\omega'^2 - \omega^2)]\mathrm{d}\omega', \tag{21}$$

so that

$$\mathrm{Re}\,A(\infty, 0) = (-2/\pi)\int_0^\infty [\mathrm{Im}\,A(\omega', 0)/\omega']\mathrm{d}\omega', \qquad \mathrm{Im}\,A(\infty, 0) = 0. \tag{22}$$

On the basis of our partitioning in §2 of the many-particle scattering problem in Rayleigh and Delbrück amplitudes, we can write down dispersion relations separately for these two scattering amplitudes. In nonrelativistic dipole approximation, $\mathrm{Re}\,A^R(\infty, 0) = -Nr_0$, with N the number of bound electrons. This is precisely the Thomas–Reiche–Kuhn sum rule (Thomas, 1925; Kuhn, 1925; Reiche & Thomas, 1925), where for $\mathrm{Im}\,A^R$ we insert (4). (Note that the single-particle form of this sum rule requires the partition we have made between A^R and A^D.) There are, however, small relativistic corrections to $\mathrm{Re}A^R(\omega, 0)$, now understood as the amplitude for scattering off the bound electrons partitioned from the amplitude for Delbrück scattering.

Another form of the dispersion relation may be written in terms of the real and imaginary parts g' and g'' of the anomalous amplitude with reference to the relativistic high-energy limit. These real quantities are defined by

$$A^R(\omega, 0) - A^R(\infty, 0) = -r_0(g' + ig''), \tag{23}$$

These anomalous scattering factors are closely related to the anomalous scattering factors f' and f'' conventionally defined in reference to the nonrelativistic high-energy limit, $-Nr_0$, as

$$g' = f' + \{N + [\mathrm{Re}\,A^R(\infty, 0)/r_0]\}, \quad g'' = f''. \tag{24}$$

The sign of our f'' differs from that commonly given in the crystallographic literature, f''_{CL} or f_2^{Henke} (see, for example, Cromer, 1983; Creagh & McAuley, 1992; Henke *et al.*, 1993) as

$$f''_{\mathrm{CL}} = f_2^{\mathrm{Henke}} = -f''. \tag{25}$$

As noted in the *Introduction*, this difference has its origins in a sign choice for the plane wave. This issue has been discussed by Ramaseshan, Ramesh & Ranganath (1975), who pointed out problems of comparing neutron and X-ray scattering where differing phase conventions are used.

The anomalous scattering factors satisfy

$$g'(\omega) = (2/\pi)\int_0^\infty [\omega' g''(\omega')/(\omega'^2 - \omega^2)]\mathrm{d}\omega'. \quad (26)$$

In the nonrelativistic case, g' reduces to the corresponding f'; the difference between g' and f' leads to a small constant correction to f' at all energies from nonrelativistic predictions. One now utilizes the optical theorem (see, for example, Nussenzveig, 1972)

$$\mathrm{Im}\, A^R(\omega, 0) = -r_0 g''(\omega) = -r_0 f''(\omega) = (\omega/4\pi c)\sigma^{\mathrm{TOT}}, \quad (27)$$

which follows from the unitarity of the S matrix, relating the total cross section for photon–atom scattering (elastic and inelastic, including absorption) to the imaginary forward elastic scattering amplitude. To lowest order in e^2, the total photoabsorption cross section for bound electrons is obtained from (4), where the bound–bound contributions are computed as

$$\sigma^{\mathrm{BBT}+}(\omega) = (2\pi^2 c r_0/\omega) \sum_{n,m>n} \omega_{nm} f_{nm} \delta(\omega - \omega_{nm}) \quad (28)$$

and

$$\sigma^{\mathrm{BBT}-}(\omega) = (2\pi^2 c r_0/\omega) \sum_{n,m<n} \omega_{nm} f_{nm} \delta(\omega - \omega_{nm}), \quad (29)$$

where f_{nm} is the oscillator strength for the transition of energy $\hbar\omega_{nm}$ of an electron from occupied state n to unoccupied state m. [The notation $m > n/m < n$ indicates the sum over unoccupied states m with energies less than or greater than the occupied state n. For ground-state atoms, the contribution from (29) is zero.] Although the total cross section at X-ray energies is dominated by absorption, primarily the atomic photoelectric effect, contributions from bound–bound transitions (see, for example, Wang & Pratt, 1983) must be included if accurate results are to be obtained from the dispersion relation for low-energy scattering. Subject to these qualifications, it should be possible to use better calculations of absorption (*i.e.* beyond IPA) or experimental data, and thereby obtain better predictions for forward elastic scattering.

From (5), the Rayleigh scattering amplitude $A^R(\omega, \theta)$ in the forward direction can be expressed as

$$A^R(\omega, 0) = (\boldsymbol{\varepsilon}_i \cdot \boldsymbol{\varepsilon}_f^*)\mathcal{M}(\omega, 0), \quad (30)$$

which can be written in terms of the anomalous scattering factors as

$$\mathcal{M}(\omega, 0) = -r_0[f(0) + f'(\omega) + if''(\omega)] \quad (31)$$

or

$$\mathcal{M}(\omega, 0) = -r_0[g(0) + g'(\omega) + ig''(\omega)]. \quad (32)$$

The real quantities f', f'' and g', g'' are called *anomalous scattering factors*. They give the deviation of the forward-scattering amplitude from the form factor and from the modified form factor, respectively.

Even though σ^{BPA} is zero until the photon energy reaches nearly $2mc^2$ and does not affect the energy dependence of the anomalous scattering factors at lower energies (determining an overall constant), the subtraction is required in order to have the integrals of (20), (22) and (26) converge at high energies, as was first noted by G. E. Brown (see Payne & Levinger, 1956). However, our interpretation of the cross section to be subtracted differs somewhat from that of Brown. In our partition of the total elastic scattering amplitude, focusing on evaluation of the diagrams in Fig. 1, our Rayleigh scattering amplitude requires the subtraction of the bound-electron pair-annihilation cross section, related to, but not the same as, the bound-electron pair-production (BPP) cross section noted by Brown. In our partition of the optical theorem, the BPP cross section is identified with the Delbrück amplitude.

With (26) and (27), we can use experimental or theoretical information regarding photoionization, photo-excitation/photode-excitation and bound-electron pair annihilation to obtain the Rayleigh scattering amplitude in the forward direction. As a consequence, the ASF formalism provides us with an approach for going beyond IPA (Zhou *et al.*, 1992*b*). Zhou, Kissel & Pratt (1992*a*) have also used these expressions to investigate the connection between Cooper minima and shape resonances in the photoionization cross section and structures in the anomalous scattering factors. Zhou, Kissel & Pratt (1992*c*) also used these expressions to devise simple computational schemes for evaluating anomalous scattering factors from ions using neutral-atom photoeffect data.

A tabulation of f', f'' for all elements at five characteristic X-ray energy lines between 5 and 22 keV was presented by Cromer & Liberman (1970*a*,*b*, 1976, 1981). In addition, these authors (Cromer & Liberman, 1970*a*; Cromer, 1983) provided a program, *FPRIME*, that computes the anomalous scattering factors for all elements $Z = 3$–98 for photon energies 1–70 keV. Henke *et al.* (1981, 1982, 1993) have made systematic tabulations of anomalous scattering factors for all elements $Z = 1$–92 for photon energies 0.05–30 keV. [Note that Henke and co-workers tabulated in terms of f_1, f_2, where $f_1(\omega) = -\mathrm{Re}\,\mathcal{M}(\omega, 0)/r_0 = N + f'(\omega)$ and $f_2(\omega) = f''(\omega)$.] No published tabulations of g', g'' now exist. However, with (24) and (25), g' and g'' may be obtained from f' and f'', as discussed in the next subsection. Within our atomic model (the relativistic Hartree–Fock–Slater potential with the Latter tail), we have tabulated g', g'' and f', f'' values for $Z = 1$–99, for photon energies 0–10 000 keV, at a variable energy grid designed to ensure two-point linear interpolation of intermediate values at an accuracy of 0.1% or better. These data as ASCII text occupy about 25 Mbytes of disk space, which can be reduced to less than 20 kbytes per

atom if the table interpolation accuracy is specified as 1% and restricted to energies of 1–100 keV; fixed-grid tables can be made much smaller. We have developed a program called *ASF* that reads these tables and computes the anomalous scattering factors (g', g''), (f', f'') or (f_1, f_2) at a specified energy, or writes a table to a disk file for a specified energy range. (Contact LK for more information regarding these data or software.)

(b) High-energy limit

In the widely used tabulations of anomalous scattering factors given by Cromer & Liberman (1970*a*,*b*, 1976, 1981), Cromer (1974, 1983) and Henke *et al.* (1981, 1982), the relativistic high-energy limit $f'(\infty)$, obtained using the electric dipole approximation, was taken as

$$f'_{\rm CL}(\infty) = \tfrac{5}{3}E_{\rm TOT}/mc^2, \tag{33}$$

where $E_{\rm TOT}$ (a negative quantity) is the difference between the total energy of the atom and that of its free constituents. However, it has been shown that higher-multipole terms give comparable contributions to f' and cannot be neglected (Jensen, 1979, 1980). With the inclusion of effects up to electric quadrupole and retardation effects, it has been shown that a *more* nearly correct value of $f'(\infty)$ is $E_{\rm TOT}/mc^2$ (Levinger, Rustgi & Okamoto, 1957; Smith, 1987).

Our numerical SM calculations have shown that the high-energy limit is given to a very high degree of accuracy by

$$f'(\infty) \simeq g(0) - N. \tag{34}$$

Therefore, in using the real anomalous scattering factors of Cromer & Liberman (1970*a*,*b*, 1976, 1981) and Cromer (1974, 1983), $f'_{\rm CL}(\omega)$, and Henke *et al.* (1981, 1982), $f_1(\omega)$, one has to make an adjustment to the high-energy limit, using

$$f'(\omega) = f'_{\rm CL}(\omega) + \delta f' = f_1(\omega) - N + \delta f', \tag{35}$$

where

$$\delta f' = f'(\infty) - f'_{\rm CL}(\infty) \simeq [g(0) - N] - \tfrac{5}{3}E_{\rm TOT}/mc^2. \tag{36}$$

These constant correction values have been tabulated for all neutral atoms by Kissel & Pratt (1990). The correction is less significant for lighter elements but is increasingly important for heavier elements. In fact, some discrepancies between older theory and experiments have been explained by this correction (Deutsch & Hart, 1988; Smith, 1987; Kissel & Pratt, 1990; Roy, Pratt & Kissel, 1993).

Please note, however, that the recent tabulation of Henke *et al.* (1993) has already included the high-energy-limit correction of Kissel & Pratt (1990); the correction of (36) should not be applied. In addition, Henke *et al.* have published a simple and accurate fit to the high-energy-limit corrections of Kissel & Pratt,

$$g(0) \simeq Z - (Z/82.5)^{2.37}. \tag{37}$$

We have verified that this simple expression reproduces our high-energy-limit values with an accuracy of 0.01% or better for the entire Periodic Table.

(c) Angle-independent ASF approximation

Upon obtaining the anomalous scattering factors g', g'' or f', f'' and thereby the forward-angle scattering amplitude, one can easily calculate the forward-angle Rayleigh scattering cross section. Equations (31) and (32) are exact if exact data for $\sigma^{\rm TOT}$ are available.

It is to be understood that the dispersion relation and the optical theorem, which are used to calculate anomalous scattering factors, are only valid for forward scattering. The validity of the use of forward-angle anomalous scattering factors at finite angles, as experiment and our S-matrix calculations have suggested, must be investigated. We mentioned earlier that relative error curves, comparing RF or MF with the S-matrix calculation, rarely show any dependence on the scattering angle for photon energy below the K-shell photoeffect threshold. This says that, in such energy regions, $\mathcal{N} \simeq 0$ in (8) or (5) is a good approximation and we may express the Rayleigh scattering amplitude at finite angle θ in terms of $\mathcal{M}$,

$$A^R \simeq (\boldsymbol{\varepsilon}_i \cdot \boldsymbol{\varepsilon}_f^*)\mathcal{M}(\omega, \theta), \tag{38}$$

and define anomalous scattering factors at a finite angle as the difference between the reduced Rayleigh scattering amplitude $\mathcal{M}(\omega, \theta)$ and the form factor or modified form factor,

$$\mathcal{M}(\omega, \theta) = -r_0[f(q) + f'(\omega, \theta) + if''(\omega, \theta)] \tag{39}$$

or

$$\mathcal{M}(\omega, \theta) = -r_0[g(q) + g'(\omega, \theta) + ig''(\omega, \theta)]. \tag{40}$$

Numerical calculations have shown that the finite-angle anomalous scattering factors defined above are insensitive to the scattering angle θ for photon energies below the K-shell threshold. So we may assume that the finite-angle anomalous scattering factors are angle-independent, that is,

$$f'(\omega, \theta) = f'(\omega), \quad f''(\omega, \theta) = f''(\omega), \tag{41}$$

or

$$g'(\omega, \theta) = g'(\omega), \quad g''(\omega, \theta) = g''(\omega). \tag{42}$$

Although our numerical calculations show that the anomalous scattering factors exhibit angle dependence, especially for high momentum transfer for high Z, we utilize the approximation of angle-independent anomalous scattering factors for all energies. We have not yet

discovered a simple expression for modeling the angle dependence of anomalous scattering factors that is a significant improvement for all Z, energies and angles. We are currently exploring use of analytic Coulomb K-shell predictions as a means of providing improved angular distributions.

Equations (39) and (40) are not equivalent at finite angles, unlike the situation for forward-angle scattering, where the g', g'' and f', f'' predictions give identical results if the same photoabsorption data are used. The angle-independent g', g'' form is a better choice for high-energy large-angle scattering (*i.e.* high momentum transfer) for high Z because the finite high-energy limit of f', although small compared to the forward-angle value of $f(0)$, dominates the real part of the scattering amplitude at large angles giving very poor predictions.

(*d*) *MF + ASF approximation*

The Rayleigh scattering amplitude in the modified-form-factor with angle-independent anomalous-scattering-factor (MF+ASF) approximation is

$$A^{\mathrm{MF+ASF}}(\omega, 0) = -r_0(\boldsymbol{\varepsilon}_i \cdot \boldsymbol{\varepsilon}_f^*)[g(q) + g'(\omega) + ig''(\omega)] \tag{43}$$

or, in terms of linear photon polarization,

$$\begin{aligned} A_{\parallel}^{\mathrm{MF+ASF}} &= A_{\perp}^{\mathrm{MF+ASF}} \cos\theta, \\ A_{\perp}^{\mathrm{MF+ASF}} &= -r_0[g(q) + g'(\omega) + ig''(\omega)]. \end{aligned} \tag{44}$$

For unpolarized scattering, the differential cross section in this approximation can be written as

$$\begin{aligned} \mathrm{d}\sigma^{\mathrm{MF+ASF}}/\mathrm{d}\Omega = (r_0^2/2)|g(q) + g'(\omega) \\ + ig''(\omega)|^2(1 + \cos^2\theta). \end{aligned} \tag{45}$$

To ensure the same threshold and transition-energy positions and permit a consistent comparison of simpler approximations and S-matrix predictions, we have calculated modified form factors $g(q)$, anomalous scattering factors g' g'' and S-matrix predictions all within the same relativistic Hartree–Fock–Slater potential, with the Latter tail. In our evaluation of the ASF, we accurately tabulated photoeffect cross sections for each subshell of the atom for photon energies from threshold to 300 keV (50 keV for $Z = 1$, 100 keV for $Z = 2$–8) using a code written by Scofield (see, for example, Saloman, Hubbell & Scofield, 1988) and combined these subshell cross sections to obtain the total-atom cross section. For higher photon energies, these total-atom photoeffect cross sections were smoothly joined to values from Lawrence Livermore National Laboratory's Evaluated Photon Data Library (Cullen, Chen, Hubbell, Perkins, Plechaty, Rathkopf & Scofield, 1989) resulting in tabulated total-atom photoeffect cross sections for energies from threshold to 10^8 keV. We directly evaluated bound–bound oscillator strengths (see, for example, Scofield, 1975) for the most significant bound–bound contributions to g' (over 500 transitions were included for carbon; over 1500 transitions were computed for lead). In our evaluation (26), we continued the integration above the pair-production threshold $2mc^2$ to an energy of 100 MeV. (Our anomalous scattering factors at about 1 MeV were insensitive to cutoffs above about 15 MeV.) The total-atom cross sections above $2mc^2$ were obtained using the expression

$$\sigma^{\mathrm{TOT}} = [(\sigma_K^{\mathrm{PE}} - \sigma_K^{\mathrm{BPA}})/\sigma_K^{\mathrm{PE}}]\sigma^{\mathrm{PE}}, \tag{46}$$

where σ_K^{PE} and σ_K^{BPA} are the K-shell cross sections obtained from analytic semirelativistic expressions due to Costescu, Bergstrom, Dinu & Pratt (1994). This expression is based on our assumption that the ratio of the total photoabsorption cross section (*i.e.* $\sigma^{\mathrm{PE}} - \sigma^{\mathrm{BPA}}$) to the photoeffect cross section for the K shell accurately represents the ratio for the total atom above $2mc^2$. A small sample of S-matrix calculations for energies of 1–5 MeV indicates that this is a reasonable assumption. (That is, we have made essentially no approximation in the evaluation of the photoeffect cross section at all energies 0–100 MeV. However, we have made an estimate of the bound pair-annihilation cross section. Errors in our estimate of σ_K^{BPA} will have no effect on the shape of our anomalous scattering factors well below the pair production threshold of $2mc^2$; errors in our estimate of σ_K^{BPA} can result in at most an overall small constant error in g' at lower energies).

Fig. 5 illustrates the differential Rayleigh scattering cross sections at $\theta = 90°$. The MF + ASF approximation (which includes bound pair annihilation and bound–bound transitions), (11) with A^R predicted using (44), has successfully reproduced the cross section of the SM calculation, including structures below the K-shell photoeffect threshold where the RF and MF approximations fail. Overall agreement is found between the MF + ASF approximation and the SM method for all photon energies. Quantitative comparisons between cross sections at three scattering angles $\theta = 0$, 30 and 90°, calculated in the MF + ASF approximation for carbon and lead, with cross sections obtained with the S-matrix method, have been prepared. For all elements, the MF + ASF approximation agrees with the S-matrix calculation very well in most photon energy ranges and all scattering angles, except for very high photon energies and large scattering angles as shown in Fig. 7. From Fig. 5, we see that the cross section changes its value most significantly near subshell thresholds. If the MF + ASF approximation and the SM calculation are not performed in the same potential, greater differences will result, especially for photon energies close to edges, owing to the different edge positions used in the two calculations.

When the photon energy increases, the differential cross section can no longer be described using the simple formula of (40) for large momentum transfers and the

cross sections obtained from the MF + ASF approximation for finite angles depart more and more from the S-matrix calculation, as seen in Fig. 6 for lead at $\theta = 90°$. For heavy elements, the MF + ASF approximation begins to fail for photon energies near the K-shell photoeffect threshold, except in the forward direction. Whether there exists a simple formula for finite-angle Rayleigh scattering well above the K-shell threshold where anomalous factors are not angle-independent and the $\mathcal{N}$ amplitude cannot be neglected, is still unsettled.

(e) Effects of bound–bound transitions in ASF

In calculations of the anomalous scattering factors, such as those in the ground-state neutral-atom tabulations of Cromer & Liberman (1970*a*,*b*, 1976, 1981), Cromer (1974, 1983) and Henke *et al.* (1981, 1982, 1993), the contribution from bound–bound transitions, the sum term in (28), has generally been thought of as small compared to the contribution from bound-free transitions, except very near edges, and has therefore been ignored. It was shown some time ago that, for atoms or ions with less than ten remaining bound electrons, the contribution from bound–bound transitions, especially from the $1s \rightarrow 2p$ transition, is significant and these transitions should be included in the real anomalous scattering factor, g' or f' (Wang & Pratt, 1983).

To illustrate the significance of the inclusion of bound–bound contributions in the anomalous scattering factors, we can examine the comparisons with the MF+ASF-BB approximation (MF+ASF neglecting bound–bound transitions) shown in Figs. 3–7. We see that neglect of bound–bound contributions results in a remarkable increase in the relative error for low photon energies for carbon. (A similar large increase in the low-energy error of MF+ASF-BB *versus* SM would also be expected for lead but will occur at still lower energies, not shown in these comparisons.)

Inclusion of bound–bound contributions, not only the $1s \rightarrow 2p$ transition but also smaller ones, is essential to obtain good agreement with the SM results at low photon energies and near to thresholds. To give a direct illustration, the differential cross section of carbon at $\theta = 90°$ near the K-shell threshold is shown in Fig. 5. The inclusion of bound–bound contributions makes the MF+ASF cross section converge to the SM predictions. We have also shown that, in the ion cases (Zhou *et al.*, 1990), the inclusion of contributions from the $1s \rightarrow 2p$ transition markedly improves the agreement of both g' and the cross section with the SM results for Ne ions. For heavy atoms with more than ten bound electrons, such as Xe or Pb, the inclusion of the bound-bound contribution is much less important for not-too-low and not-too-close-to-threshold photon energies. So, it is increasingly less important to include bound-bound contributions in MF+ASF for atoms or ions as the number of bound electrons increases above ten, for most photon energies.

The inclusion of bound–bound transitions is also important for satisfying the relativistic Thomas–Reiche–Kuhn (TRK: Thomas, 1925; Kuhn, 1925; Reiche & Thomas, 1925) sum rule, which is, to lowest order in e^2,

$$N \simeq (1/2\pi^2 cr_0) \int_0^\infty [\sigma^{\mathrm{PE}}(\omega') - \sigma^{\mathrm{BPA}}(\omega')]\mathrm{d}\omega' + \sum_{n,m} f_{nm} - f'(\infty). \quad (47)$$

The effect of neglecting bound–bound transitions is especially significant for low photon energies, not only for atoms with less than 10 bound electrons but also for other atoms in general because the contribution to g' or f' at low energy associated with a bound–bound transition $n \rightarrow m$ is nearly constant.

$$\lim_{E \ll E_{nm}} \{f_{nm}/[1 - (E/E_{nm})^2]\} = f_{nm}, \quad (48)$$

with f_{nm} the oscillator strength of the transition. In Fig. 8, we show the total contribution of bound–bound transitions to the TRK sum rule, (47), for all neutral ground-state atoms. Bound–bound transitions contribute 30% or more to the sum rule for atoms $Z = 1$, 3–5, 20, 21 and 56–58.

Fig. 8 exhibits a regular structure with local minima corresponding to closed-shell or nearly closed-shell atoms (^{2}He, ^{10}Ne, ^{18}Ar, ^{36}Kr, ^{46}Pd, ^{54}Xe, ^{79}Au and ^{86}Rn). A sharp rise in the total oscillator strength is observed for the elements immediately following the atoms with close-shell configurations; in lighter atoms, the extra electrons are generally added to the s state of a new shell, opening channels for strong s–p dipole transitions, and, in heavier atoms, the extra electrons enhance p–d and d–f transitions of existing incompletely filled shells. As additional electrons are added, the total oscillator strength decreases as the extra electrons fill the formerly open upper state of the transitions; eventually, the shell is closed and a new minimum in oscillator strength is reached.

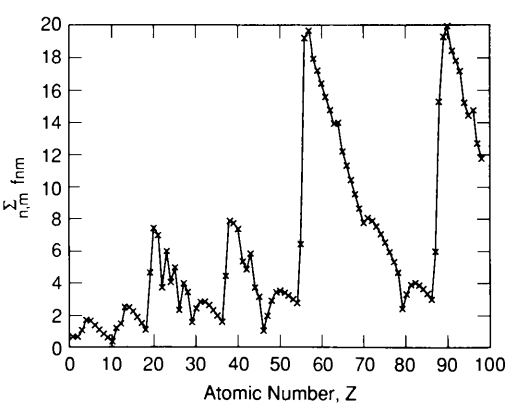

Fig. 8. Contribution of bound–bound transitions to the TRK sum rule.

(*f*) *Sample comparisons with experiment*

To give an idea of the improvements from form-factor predictions achieved by including anomalous-scattering corrections, we present the case of $\theta = 90°$ scattering of 59.54 keV photons in Fig. 9. Here we compare predictions in MF and MF+ASF approximations with measurements by various authors that span most of the Periodic Table. We can see significant differences between MF and MF+ASF predictions, especially for atomic numbers around $Z = 70$ where the photon energy crosses the K-shell photoeffect threshold.

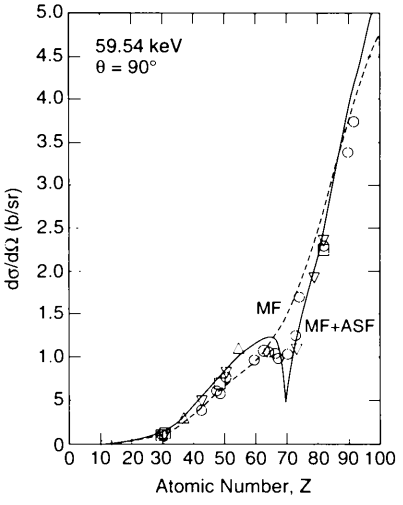

Fig. 9. Comparison of our MF (broken line) and MF+ASF (solid line) predictions for the differential cross section at $\theta = 90°$ for 59.54 keV photons with experiment (▽ Schumacher & Stoffregen, 1977; □ Eichler & de Barros, 1985; △ Smend & Czerwinski, 1986; ○ Govinda Nayak, Siddappa, Balakrishna & Lingappa, 1992).

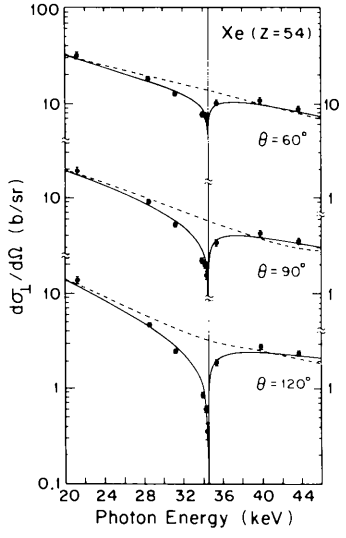

Fig. 10. Comparison of our MF (broken lines) and MF+ASF (solid lines) predictions for the linearly polarized differential cross section, near the K-shell photoeffect threshold of xenon, with the experiment of Smend *et al.* (1987).

As a second example, we show in Fig. 10 comparisons with a polarized scattering experiment that involve photon energies near the xenon K-shell photoeffect threshold (at about 34.5 keV). In this example, the cross section is shown for scattering of photons with linear polarization perpendicular to the scattering plane, $d\sigma_\perp/d\Omega$, at three angles $\theta = 60$, 90 and 120°. We observe that agreement is generally quite good between the measurements of Smend *et al.* (1987) and the MF+ASF predictions.

As a more stringent test, we show in Figs. 11–15 a comparison of our predictions of f' and the recent experiments of Stanglmeier, Lengeler, Weber, Göbel & Schuster (1992). We observe generally good agreement between theory and experiment for photon energies not too near to thresholds for the K-shell thresholds of lighter atoms. Less satisfactory agreement is seen for the L-shell thresholds of the heavy atoms. For tantalum and gold, the agreement is generally good for higher energies, poorer for lower energies; the sign of the low-energy discrepancy is different in the two cases. The agreement for platinum is systematically poor, with the greatest disagreement for the lower energies.

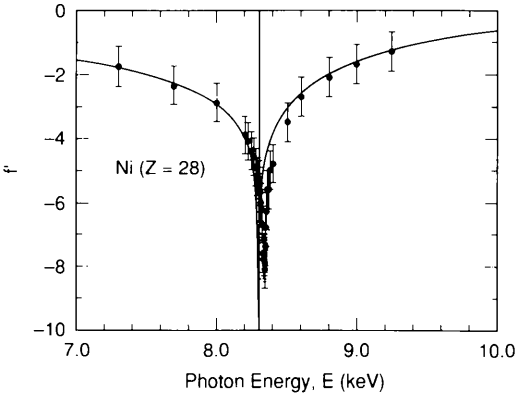

Fig. 11. Comparison of our f' predictions with the measurements of Stanglmeier *et al.* (1992) for nickel.

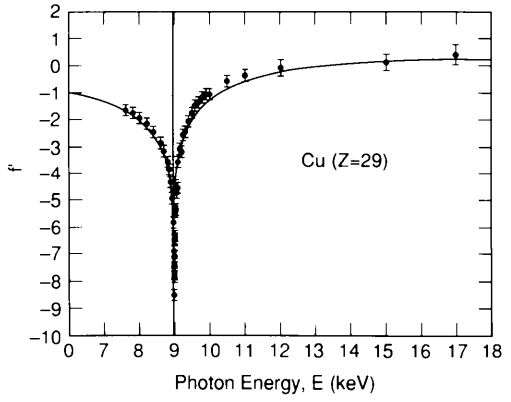

Fig. 12. Same as Fig. 11, for copper.

(g) Concluding remarks on the validity of the MF+ASF approximation

From Figs. 3–7, we conclude that:

(i) For all photon energies below the K-shell photoeffect threshold, the differential cross section of Rayleigh scattering predicted by the MF+ASF method works very well (errors less than about 5%).

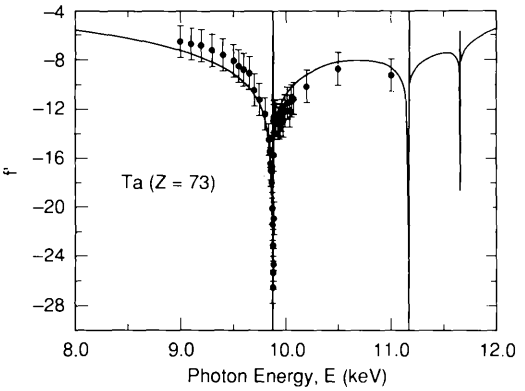

Fig. 13. Same as Fig. 11, for tantalum.

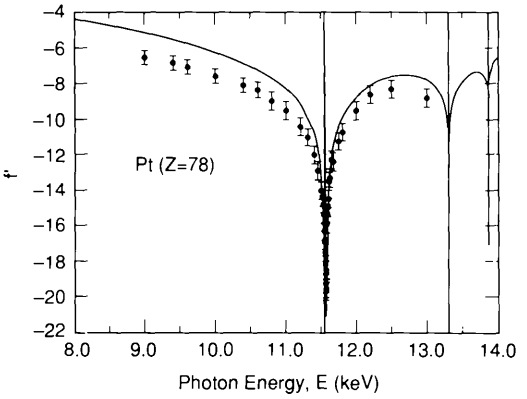

Fig. 14. Same as Fig. 11, for platinum.

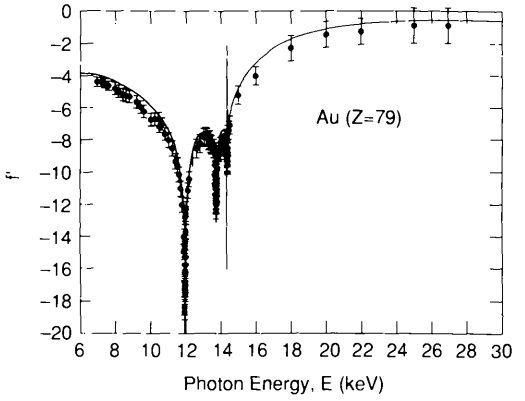

Fig. 15. Same as Fig. 11, for gold.

(ii) Above the K-shell threshold, the differential cross section obtained in the MF+ASF approximation is very good for all angles in low-Z elements and for small-angle scattering in high-Z elements.

(iii) The predicted differential cross section in MF+ASF approximation fails at large angles for photon energies well above the K-shell photoeffect threshold.

(iv) For low-Z atoms with less than ten bound electrons, the inclusion of the contributions from bound–bound transitions to g' is crucial for low photon energies, while for intermediate and heavy elements it is less important in the X-ray regime. (Bound–bound transitions remain important at low energies for all Z.)

(v) For all photon energies, the MF+ASF approximation, with the bound–bound contribution properly included, works very well for the total angle-integrated cross section.

We stress that our comparison between theories has been made within a single atomic model and that all calculations (*i.e.* the SM, MF and ASF calculations, including the atomic photoeffect and the bound–bound transition calculations) are performed in the same IPA potential. Our aim here has been to investigate how accurately simpler and more approximate theories can duplicate features of the SM calculation for a given model potential. This can give insight regarding the utility of such approaches when experimental data, rather than SM data in a model, are used. Any differences in atomic potentials that would shift atomic thresholds between the SM calculation and the ASF calculation will result in significantly larger discrepancies for photon energies near to edges.

6. Beyond the IPA model

Our calculations have been performed for Rayleigh scattering from an isolated and neutral ground-state atom within the framework of the independent-particle approximation. This approach is insufficient when correlations among electrons become important (such as for very low photon energies or very close to thresholds) or when the atom is strongly affected by an environment (such as in the solid state or a plasma).

Since Rayleigh scattering is, in fact, a many-electron process, incorporation of correlation effects can proceed by one of several existing approaches, such as many-body perturbation theory (Garvin, Brown, Carter & Kelly, 1983) or random phase approximation (Amusia, Ivanov & Chernysheva, 1981), although no direct calculation of scattering has been attempted *via* these approaches. Alternatively, in the time-dependent local-density approximatation method (TDLDA), which includes electron correlations, the atomic polarizability can be calculated and hence the anomalous scattering factors can be obtained (Doolen & Liberman, 1987). Another approach is to directly calculate the higher-order S-matrix elements, such as fourth-order S-matrix elements

(Lin *et al.*, 1975), which can include diagrams representing some electron–electron correlations resulting from direct photon exchange.

A convenient indirect way to incorporate electron correlation effects in Rayleigh scattering is through (26) and (27), since the optical theorem and dispersion relations are fundamental relations of physical processes of much more general validity. One can calculate the anomalous scattering factors utilizing experimental photoionization cross sections (Barkyoumb & Smith, 1990; Barkyoumb, Morrison & Smith, 1990) or use more sophisticated calculations beyond IPA, such as the relativistic random phase approximation (Zhou *et al.*, 1992*b*). There is always a problem of consistency, since the equations require data from all energies while experiment or more sophisticated theory is available for limited ranges. Sum rules such as (47) provide important tests.

In Figs. 16 and 17, we focus on a near-threshold comparison for the K shell of nickel. Our independent-particle-approximation (IPA) relativistic self-consistent

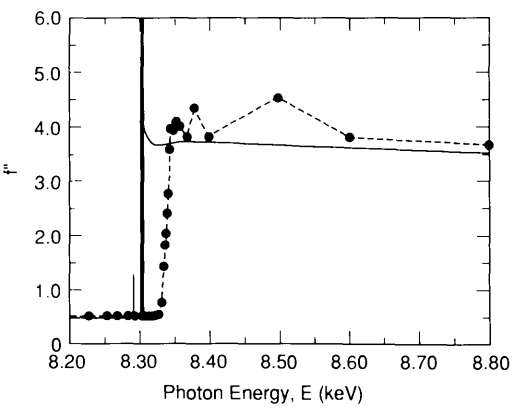

Fig. 16. Detailed comparison of f'' predictions close to the K-shell photoeffect threshold for nickel: our unmodified IPA predictions (solid line); experimental values of Stanglmeier *et al.* (1992) (●); IPA predictions incorporating near-edge experimental information (broken line).

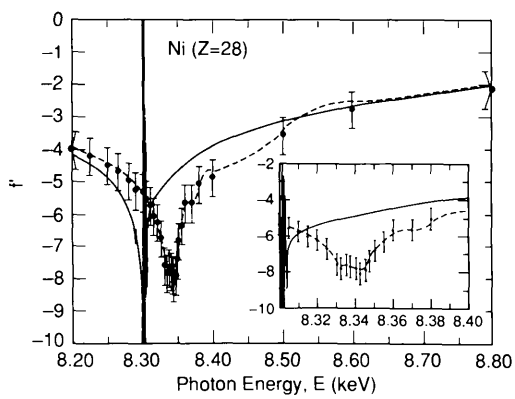

Fig. 17. Same as Fig. 16, for f'.

atomic model does not precisely predict the threshold observed in the experiment. As a consequence, our unmodified predictions (the solid curves in the figures) are observed to be displaced in energy for the measurements. An *ad hoc* modification to our predictions (broken curves in the figures) results from the replacement of our IPA photoabsorption data (both photoeffect data and bound–bound transition data) for photon energies of 7.3–9.25 keV with values measured by Stanglmeier *et al.* (1992). The resulting IPA plus near-edge photoabsorption data can be used in (27) and (26) to obtain the broken curves in Figs. 16 and 17. We observe a dramatic improvement in the agreement between these modified predictions and experiment even though the spacing of the data from Table 3 of Stanglmeier *et al.* (1992) is not dense enough to fully characterize the near-edge structure and extended X-ray absorption fine-structure spectroscopy in the photoabsorption data. Our modified predictions also satisfy the TRK sum rule, (47), to a high degree of accuracy, yielding a numerical value of 28.001, which differs by less than 0.01% from the correct value of 28.

Thus, we have demonstrated that detailed and accurate measurements of the near-edge photoabsorption data can be used to improve IPA ASF predictions. But this level of experimental information is not systematically available for all elements and ions in the Periodic Table. As a consequence, we are also exploring other *ad hoc* modifications of our IPA predictions that use less detailed experimental information. In particular, we are currently investigating the utility of energy scaling procedures that depend only on the use of experimental binding energies, available for most subshells of most neutral atoms.

7. Concluding remarks

We have carried out a systematic assessment of the relativistic form-factor (RF), modified-form-factor (MF) and anomalous-scattering-factor (ASF) approximations, and their validity in comparison with the second-order S-matrix (SM) calculation, for some representative atoms. In general, RF and MF are high-photon-energy and small-momentum-transfer approximations. They provide good predictions of small-angle differential cross sections for photon energies above the K-shell photoeffect threshold, while they fail at all angles for photon energies below the K threshold and at large angles for photon energies well above the K threshold for high-Z elements. Both RF and MF can provide good predictions for the angle-integrated cross section above the K threshold but not below. The MF value in the forward direction is very close to the correct high-energy limit of the forward-angle Rayleigh scattering amplitude. The use of MF with angle-independent ASF (MF+ASF) provides an accurate and efficient way to predict Rayleigh scattering cross sections for all angles for photon energies near and below

the K-shell photoeffect threshold, though the angle-independent assumption for ASF fails for finite angles at photon energies well above the K threshold for high-Z elements. The commonly employed high-energy limit $f'_{CL}(\omega) = \frac{5}{3}E_{TOT}/mc^2$, which was derived within the dipole approximation, is inadequate and the more correct high-energy limit $f'(\infty) \simeq g(0) - N$ has to be used, especially for heavy atoms. For atoms with less than ten electrons, the bound–bound contribution to the real ASF is significant and should be included, while for heavier atoms the bound-bound contributions can still be significant for very low energies. After incorporating both the bound–bound contributions and the correct higher-energy limit, we have shown that the Rayleigh-scattering cross sections predicted by MF+ASF, calculated in the same potential as in the SM calculation, agree with the SM results within 5% for all angles and all atoms, for photon energies below the K-shell photoeffect threshold. In comparisons of our ASF predictions with experiment, we observe that independent-particle-approximation (IPA) isolated-atom predictions can show serious disageement with measurements, especially near thresholds. The origin of the disagreement is not the ASF procedure itself but the validity of the photoabsorption data used in the procedure. Marked improvements in ASF predictions have been demonstrated through the incorporation of experimental information.

This work is supported in part by US National Science Foundation under grants PHY90-05763, PHY93-07478 and INT88-12627, and in part under the auspices of the US Department of Energy by Lawrence Livermore National Laboratory under contract number W-7405-ENG-48.

References

AMUSIA, M. YA., IVANOV, V. K. & CHERNYSHEVA, L. V. (1981). *J. Phys. B*, **14**, L19–L23.

BARKYOUMB, J. H., MORRISON, T. I. & SMITH, D. Y. (1990). *Phys. Lett. A*, **143**, 462–466.

BARKYOUMB, J. H. & SMITH, D. Y. (1990). *Phys. Rev. A*, **41**, 4863–4867.

BASAVARAJU, G., KANE, P. P. & VARIER, K. M. (1979). *Pramana*, **12**, 665–678.

BRENNER, S., BROWN, G. E. & WOODWARD, J. B. (1955). *Proc. R. Soc. London Ser. A*, **227**, 59–72.

BROWN, G. E. & MAYERS, D. F. (1956). *Proc. R. Soc. London Ser. A*, **234**, 387–390.

BROWN, G. E. & MAYERS, D. F. (1957). *Proc. R. Soc. London Ser. A*, **242**, 89–95.

BROWN, G. E., PEIERLS, R. E. & WOODWARD, J. B. (1955). *Proc. R. Soc. London Ser. A*, **227**, 51–58.

COSTESCU, A., BERGSTROM, P. M. JR, DINU, C. & PRATT, R. H. (1994). *Phys. Rev. A*, **50**, 1390–1398.

CREAGH, D. C. & MCAULEY, W. J. (1992). *International Tables for Crystallography*, Vol. C, edited by A. J. C. WILSON, pp. 206–222. Dordrecht: Kluwer Academic Publishers.

CROMER, D. T. (1974). *International Tables for X-ray Crystallography*, Vol. IV, edited by J. A. IBERS & W. C. HAMILTON, pp. 148–150. Birmingham: Kynoch Press. (Present distributor Kluwer Academic Publishers, Dordrecht.)

CROMER, D. T. (1983). *J. Appl. Cryst.* **16**, 437.

CROMER, D. T. & LIBERMAN, D. A. (1970*a*). *Relativistic Calculation of Anomalous Scattering Factors for X-rays*. Los Alamos Scientific Laboratory Report LA-4403, Los Alamos, NM, USA.

CROMER, D. T. & LIBERMAN, D. A. (1970*b*). *J. Phys. Chem.* **53**, 1891–1989.

CROMER, D. T. & LIBERMAN, D. A. (1976). *Acta Cryst.* A**32**, 339–340.

CROMER, D. T. & LIBERMAN, D. A. (1981). *Acta Cryst.* A**37**, 267–268.

CULLEN, D. E., CHEN, M. H., HUBBELL, J. H., PERKINS, S. T., PLECHATY, E. F., RATHKOPF, J. A. & SCOFIELD, J. H. (1989). *Tables and Graphs of Photon-Interaction Cross Sections from* 10 eV *to* 100 GeV *Derived from the LLNL Evaluated Photon Data Library (EPDL)*. Lawrence Livermore National Laboratory Report UCRL-50400, Vol. 6, Rev. 4, Livermore, CA, USA.

DEUTSCH, M. & HART, M. (1988). *Phys. Rev. B*, **37**, 2701–2703.

DOOLEN, G. & LIBERMAN, D. (1987). *Phys. Scr.* **36**, 77–79.

EICHLER, J. & DE BARROS, S. (1985). *Phys. Rev. A*, **32**, 789–792.

FLORESCU, V. & GAVRILA, M. (1976). *Phys. Rev. A*, **14**, 211–235.

FRANZ, W. (1935). *Z. Phys.* **95**, 652–668.

FRANZ, W. (1936). *Z. Phys.* **98**, 314–320.

GARVIN, L. J., BROWN, E. R., CARTER, S. L. & KELLY, H. P. (1983). *J. Phys. B*, **16**, L269–L274.

GOLDBERGER, M. L. & LOW, F. E. (1968). *Phys. Rev.* **176**, 1778–1781.

GOVINDA NAYAK, N., SIDDAPPA, K., BALAKRISHNA, K. M. & LINGAPPA, N. (1992). *Phys. Rev. A*, **45**, 4490–4493.

HENKE, B., GULLIKSON, E. M. & DAVIS, J. C. (1993). *At. Data Nucl. Data Tables*, **54**, 181–342.

HENKE, B., LEE, P., TANAKA, T. J., SHIMABUKURO, R. L. & FUJIKAWA, B. K. (1981). *Low Energy X-ray Diagnostics* – 1981 *(Monterey)*. *AIP Conf. Proc.* No. 75, edited by D. T. ATTWOOD & B. L. HENKE, pp. 340–388. New York: American Institute of Physics.

HENKE, B., LEE, P., TANAKA, T. J., SHIMABUKURO, R. L. & FUJIKAWA, B. K. (1982). *At. Data Nucl. Data Tables*, **27**, 1–144.

HUBBELL, J. H. & ØVERBØ, I. (1979). *J. Phys. Chem. Ref. Data*, **8**, 69–109.

HUBBELL, J. H., VEIGELE, W. J., BRIGGS, E. A., BROWN, R. T., CROMER, D. T. & HOWERTON, R. J. (1975). *J. Phys. Chem. Ref. Data*, **4**, 471–538; erratum (1977), **6**, 615–616.

ICE, G. E., CHEN, M. H. & CRASEMANN, B. (1978). *Phys. Rev. A*, **17**, 650–658.

JAMES, R. W. (1962). *The Optical Principles of the Diffraction of X-rays*. London: Bell.

JENSEN, M. S. (1979). *Phys. Lett.* **74A**, 41–44.

JENSEN, M. S. (1980) *J. Phys. B*, **13**, 4337–4344.

JOHNSON, W. R. & CHENG, K. T. (1976). *Phys. Rev. A*, **13**, 692–698.

JOHNSON, W. R. & FEIOCK, F. D. (1968). *Phys. Rev.* **168**, 22–31.

KANE, P. P., KISSEL, L., PRATT, R. H. & ROY, S. C. (1986). *Phys. Rep.* **140**, 75–159.

KANE, P. P., MAHAJANI, J., BASAVARAJU, G. & PRIYADARSHINI, A. K. (1983). *Phys. Rev. A*, **28**, 1509–1516.

KARLE, J. (1989). *Phys. Today*, **42**, No. 6, 22–29.

KISSEL, L. (1977). PhD thesis, Univ. of Pittsburgh, USA.

KISSEL, L. & PRATT, R. H. (1985). *Atomic Inner-Shell Physics*, edited by B. CRASEMANN, pp. 465–532. New York: Plenum Press.

KISSEL, L. & PRATT, R. H. (1990). *Acta Cryst.* A**46**, 170–175.

KISSEL, L., PRATT, R. H. & ROY, S. C. (1980). *Phys. Rev. A*, **22**, 1970–2004.

KUHN, W. (1925). *Z. Phys.* **33**, 408–412.

LEVINGER, J. S. (1952). *Phys. Rev.* **87**, 656–662.

LEVINGER, J. S., RUSTGI, M. L. & OKAMOTO, K. (1957). *Phys. Rev.* **106**, 1191–1194.

LIBERMAN, D. A., CROMER, D. T. & WABER, J. T. (1971). *Comput. Phys. Commun.* **2**, 107–113.

LIN, C. P., CHENG, K. T. & JOHNSON, W. R. (1975). *Phys. Rev. A*, **11**, 1946–1956.

MÜCKENHEIM, W. & SCHUMACHER, M. (1980). *J. Phys. G*, **6**, 1237–1250.

NUSSENZVEIG, H. M. (1972). *Causality and Dispersion Relations*. New York: Academic Press.

PARKER, J. C. & PRATT, R. H. (1984). *Phys. Rev. A*, **29**, 152–158.

PAYNE, W. B. & LEVINGER, J. S. (1956). *Phys. Rev.* **101**, 1020–1026.
PRATT, R. H., KISSEL, L. & BERGSTROM, P. M. JR (1994). *X-ray Anomalous (Resonance) Scattering: Theory and Experiment*, edited by K. FISCHER, G. MATERLIK & C. SPARKS. Amsterdam: Elsevier/North Holland.
RAMASESHAN, F., RAMESH, T. G. & RANGANATH, G. S. (1975). *Anomalous Scattering*, edited by F. RAMASESHAN & S. C. ABRAHAMS, pp. 139–161. Copenhagen: Munksgaard.
REICHE, F. & THOMAS, W. (1925). *Z. Phys.* **34**, 510–525.
ROY, S. C. (1991). *Phys. Rev. A*, **43**, 6393–6394.
ROY, S. C., KISSEL, L. & PRATT, R. H. (1983). *Phys. Rev. A*, **27**, 285–290.
ROY, S. C., PRATT, R. H. & KISSEL, L. (1993). *Rad. Phys. Chem.* **41**, 725–738.
ROY, S. C., SARKAR, B., KISSEL, L. & PRATT, R. H. (1987). *Nucl. Instrum. Methods A*, **255**, 66–67.
ROY, S. C., SARKAR, B., PRATT, R. H. & KISSEL, L. (1986). *Phys. Rev. A*, **34**, 1178–1187.
RULLHUSEN, P., MÜCKENHEIM, W., SMEND, F., SCHUMACHER, M., BERG, G. P. A., MORK, K. & KISSEL, L. (1981). *Phys. Rev. C*, **23**, 1375–1383.
SAKURAI, J. J. (1967). *Advanced Quantum Mechanics*. Reading: Addison-Wesley.
SALOMAN, E. B., HUBBELL, J. H. & SCOFIELD, J. H. (1988). *At. Data Nucl. Data Tables*, **38**, 1–197.
SCHAUPP, D., SCHUMACHER, M., SMEND, F. & RULLHUSEN, P. (1983). *J. Phys. Chem. Ref. Data*, **12**, 467–512.
SCHUMACHER, M. & STOFFREGEN, A. (1977). *Z. Phys. A*, **283**, 15–19.
SCOFIELD, J. H. (1975). *Atomic Inner-Shell Processes*, edited by B. CRASEMANN, pp. 265–292. New York: Academic Press.
SMEND, F. & CZERWINSKI, H. (1986). *Z. Phys. D*, **1**, 139–140.
SMEND, F., SCHAUPP, D., CZERWINSKI, H., SCHUMACHER, M., MILLHOUSE, A. H. & KISSEL, L. (1987). *Phys. Rev. A*, **36**, 5189–5199.
SMITH, D. Y. (1987). *Phys. Rev. A*, **35**, 3381–3387.
SOMMERFELD, A. (1939). *Atombau and Spektrallinien*, Vol. 2. Braunschweig: Vieweg.
STANGLMEIER, F., LENGELER, B., WEBER, W., GÖBEL, H. & SCHUSTER, M. (1992). *Acta Cryst.* A**48**, 626–639.
THOMAS, W. (1925). *Naturwissesnschaften*, **13**, 627.
WANG, M. S. & PRATT, R. H. (1983). *Phys Rev. A*, **28**, 3115–3116.
ZHOU, B. (1991). PhD thesis, Univ. of Pittsburgh, USA.
ZHOU, B., KISSEL, L. & PRATT, R. H. (1992*a*). *Phys Rev. A*, **45**, 2983–2988.
ZHOU, B., KISSEL, L. & PRATT, R. H. (1992*b*). *Phys. Rev. A*, **45**, 6906–6909.
ZHOU, B., KISSEL, L. & PRATT, R. H. (1992*c*). *Nucl. Instrum Methods B*, **66**, 307–312.
ZHOU, B., PRATT, R. H., ROY, S. C. & KISSEL, L. (1990). *Phys. Scr.* **41**, 495–498.

Acta Cryst. (1995). A**51**, 288–294

Reformulation of the Statistical Theory of Dynamical Diffraction in the Case $E = 0$

BY J. P. GUIGAY

Laboratoire Louis Néel, BP 166, 38042 *Grenoble CEDEX* 9, *France*

AND F. N. CHUKHOVSKII

Institute of Crystallography, Russian Academy of Science, Moscow 117333, *Russia*

(*Received* 8 *March* 1994; *accepted* 21 *September* 1994)

Abstract

The statistical theory of dynamical diffraction, in the case $E = 0$, for which there is no long-range order, is reformulated with rigorous boundary conditions. The presence of a coherent forward-diffracted wave along the boundary of the influence region in the spherical-wave approach is taken into account. The integrated reflectivity is calculated in the case of Laue geometry and is found to be significantly different from the result of the previous formulations if $\chi^2\tau T > 1$ (χ is the reciprocal of the extinction distance, τ is the correlation length of the lattice imperfection and T is the crystal thickness along the incident direction).

1. Introduction

Following Kato (1980), the Bragg diffracted intensity from a randomly distorted crystal contains a coherent part and an incoherent part, which are related to the statistical averages and to the statistical fluctuations of the wave amplitudes, respectively. Further developments and some modifications of the original treatment of Kato (1980) have been proposed by the various authors quoted in the reference list of the present paper, and its applicability to some experimental data has been discussed recently by Schneider, Bouchard, Graf & Nagasawa (1992), Takama (1993) and Takama & Harida (1994).

A more general form of the statistical theory, based on wave equations more rigorous than the Takagi–Taupin equations used below, has also been proposed by Kato (1991), but this new advanced development is not considered in the present paper. The theory based on the Takagi–Taupin equations can itself be reformulated in a more complete form, especially by reconsidering the boundary conditions along the edges of the Borrmann fan. This was first done for the coherent waves (Guigay & Chukhovskii, 1992; see also Kato, 1994). The purpose of the present paper is to continue this reformulation for

ISSN 0108-7673